Structures 60 (2024) 105972

Contents lists available at ScienceDirect

Structures

journal homepage: www.elsevier.com/locate/structures

# The geometry of principal symmetric structures

Davide Pellis [a,*], Helmut Pottmann [b]

[a] ISTI - CNR, Via Giuseppe Moruzzi 1, Pisa, 56127, Italy
[b] KAUST, 4700 King Abdullah University of Science and Technology, Thuwal, 23955-6900, Saudi Arabia

ARTICLE INFO

*Keywords:*
Gridshells
Structural optimization
Architectural geometry

ABSTRACT

We introduce a novel class of quadrilateral gridshell structures in axial force equilibrium where rods are aligned symmetrically with the principal stress directions of a limit membrane shell. These structures exhibit a distinctive property where the axial forces in the four connected rods at each node are nearly equal. This characteristic enables a more uniform distribution of forces within the structure, particularly in cases where stresses exhibit significant anisotropy. In contrast, conventional gridshells often result in numerous rods remaining nearly unloaded in such scenarios. We begin by studying the equilibrium of rod networks that are symmetric to principal stress directions. Next, we explore the geometric properties of these networks in relation to the isotropic geometry of their Airy stress surface. We introduce then a computational pipeline for designing principal symmetric structures through quadrilateral remeshing of a surface in membrane equilibrium and subsequent optimization. Finally, we present some of the achieved results.

## 1. Introduction

Gridshell trusses provide an efficient solution to building shell structures, combining strength with a lightweight architectural design. Indeed, by transmitting loads through axial stresses within their rods, these structures maximize the utilization of structural material.

Among all gridshells, quadrilateral configurations are especially well-suited for manufacturing. Firstly, compared to triangular configurations, they enable connections where four rods meet at joints instead of six. Furthermore, when rods follow the principal curvature directions of the underlying surface, we attain flat cladding panels and joint connections that align along a common axis, streamlining the production process (see [1]).

From a mechanical perspective, a common approach to designing quadrilateral gridshell trusses is to follow the principal stress lines of a membrane shell. In this way, we achieve an orthogonal framework in axial equilibrium. It has also been shown in [2] that such structures are the ones that minimize the usage of structural material in tension-compression areas on a given shape in membrane equilibrium. However, when the principal stresses of the membrane exhibit significant anisotropy, aligning the rods with the principal stress directions can cause many rods to remain largely unloaded in the direction of lower stress, as shown in Fig. 2. When using rods with a constant cross-section, this leads to suboptimal material usage. If rods with similar forces are clustered into a limited collection of cross-sections, the majority of joints will involve connecting different profiles, thereby increasing manufacturing complexity.

In this paper, we introduce a new class of quadrilateral gridshell trusses, called principal symmetric gridshells, characterized by nearly equal axial forces at each joint. A distinctive feature of these gridshells is that, despite variations in axial forces within the structure, the force distribution remains remarkably homogeneous. As a consequence, a reduced collection of cross-sections can be employed, and joints exhibit a majority of connected beams sharing identical profiles, reducing fabrication complexity and material waste. It turns out that such gridshells must follow two specific directions that are symmetric to the principal stress directions of a tension-only or a compression-only membrane.

### 1.1. Related work

This study is situated in the broader field of gridshell design and optimization, which has been extensively reviewed in [3]. Our approach leverages the separation of horizontal and vertical equilibrium and utilizes the polyhedral Airy stress potential as a discretization of a continuum, drawing upon the methodological insights provided in [4] and [5]. Strubecker [6] was the first to realize the connection between equilibrium of a 2D elastic body and geometric properties of the associated Airy stress surface in isotropic geometry. In this context, Vouga et al. [7] further leveraged the connections between statics and discrete differential geometry.

Regarding the layout design of gridshells, the works of Mitchell [8] and Kilian et al. [2] investigated the use of quadrilateral meshes aligned

* Corresponding author.
*E-mail address:* davide.pellis@isti.cnt.it (D. Pellis).

https://doi.org/10.1016/j.istruc.2024.105972
Received 20 October 2023; Received in revised form 16 January 2024; Accepted 25 January 2024
Available online 29 January 2024

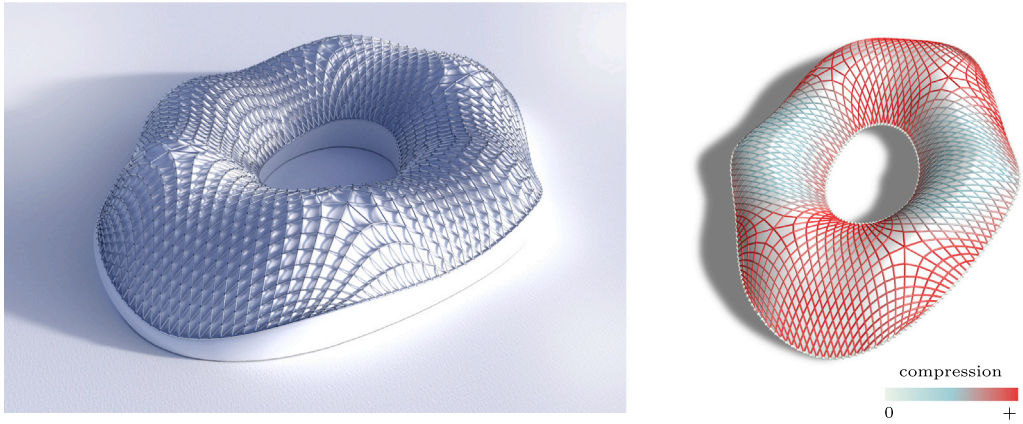


**Fig. 1.** A principal symmetric gridshell and its axial forces under a vertical homogeneous load (*right*).

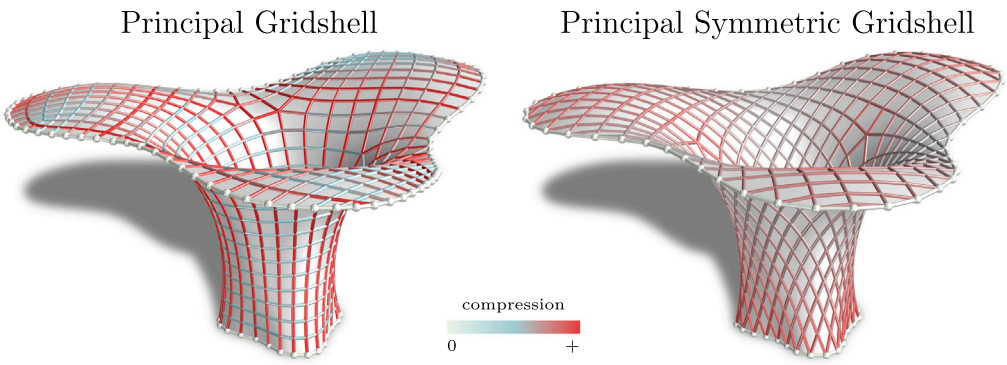


**Fig. 2.** On the *left*, a gridshell aligned with principal stress directions. Many rods remain almost unloaded. On the *right*, a principal symmetric gridshell. At each node, the distribution of axial forces is more homogeneous.

with principal stresses as statically-optimal gridshells. These works build upon the pioneering finding of A.G. Michell on trusses at the limit of economy [9]. Furthermore, gridshells aligned with both principal stresses and principal curvatures of a membrane surface have been addressed in [10], while structures symmetric to principal stress directions have been previously introduced by Schling and colleagues [11] on shapes with rotational symmetry.

The geometric properties and manufacturing implications of quadrilateral gridshells have been extensively studied in the field of architectural geometry, as surveyed in [12]. In this context, Pellis et al. [13] introduced gridshells that are symmetric to principal curvature directions, rather than principal stress directions, and investigated their potential for use in architectural panelization.

### 1.2. Overview and contributions

This paper builds upon and completes our previous preliminary work on principal symmetric structures [14] with a geometric characterization in terms of isotropic geometry. In Section 2, we begin with a brief overview of truss equilibrium at the limit of refinement, while considering its relationship with the Airy stress surface. Additionally, we introduce the concept of the Airy stress surface in the context of isotropic geometry. In Section 3, we start exploring the properties of principal symmetric structures in two dimensions and exploit their properties in isotropic geometry. In Section 4, we extend our geometric interpretation to gridshell structures under vertical loading conditions. Finally, in Section 5, we outline our computational design pipeline for the creation of principal symmetric gridshells with additional implementation details and show new results.

## 2. Equilibrium of 2D trusses

In this section, we introduce the equilibrium of trusses in 2D. Our approach involves a refinement process of the truss, which eventually converges to a "truss-like continuum" where the mechanical state can be described using the Cauchy stress tensor. First, we show that the equilibrium of a 2D truss implies the existence of a polyhedron that represents its axial forces. Next, we analyze the problem in the continuum setting where the polyhedron converges to a Airy stress surface. Finally, we study a quadrilateral truss at the limit of refinement as a network of curves on the Airy stress surface.

### 2.1. Discrete equilibrium

Let us consider a two dimensional truss in the $xy$-plane, with members corresponding to the edges of a mesh $M$ with vertices $\mathbf{v}_i = (x_i, y_i)$, where loads and support reactions are applied at boundary vertices. Let $\mathbf{f}_{ij}$ be the force exerted by the oriented bar $\mathbf{v}_i - \mathbf{v}_j$ on the vertex $\mathbf{v}_i$. If the system is in axial equilibrium, at each unsupported vertex $\mathbf{v}_i$ we have

$$\sum_{j\sim i} \mathbf{f}_{ij} = 0, \tag{1}$$

where with $j \sim i$ we denote all the vertices $j$ connected with the vertex $i$.

As shown by Maxwell [15], for such a truss we can construct a *force polyhedron* $P$ with planar faces, whose edges and vertices coincide in the $xy$ projection with the mesh $M$, in the following way. Let the polyhedron $P$ be described by the piece-wise linear function $z = \phi(x, y)$, and let $\phi|_f$ be the restriction of the function to the face $f$. Each face $f$ of $P$ lies then on a plane with gradient $\nabla\phi|_f$. Let $f_l$ and $f_r$ be the left and right faces of the oriented edge $\mathbf{v}_i - \mathbf{v}_j$. The continuity of the plane

faced polyhedron $P$ implies that the difference vectors $\nabla\phi|_{f_r} - \nabla\phi|_{f_l}$, which are oriented orthogonally to each edge $\mathbf{v}_i - \mathbf{v}_j$, form a closed loop around each interior vertex $\mathbf{v}_i$. Let then $R$ be the counterclockwise 90° rotation matrix in the $xy$-plane. By setting $\mathbf{f}_{ij} = R(\nabla\phi|_{f_r} - \nabla\phi|_{f_l})$, the equilibrium of Eq. (1) is then ensured at each interior vertex by the existence of the force polyhedron $P$. Forces exerted at boundary vertices can be represented through the incorporation of a boundary strip consisting of planar faces intersecting along the lines of action of the applied forces. In cases where adjacent boundary vertices are free of external loads, they naturally align within a shared plane. The closure of this strip ensures the overall global equilibrium of the structure. This construction is uniquely defined up to vertical translations and shearing. For further details see [15], [4] and [7].

### 2.2. Equilibrium of a 2D continuum

Let us now consider a refinement process that increases the density of a 2D truss. From a mechanical perspective, as the refinement limit is reached, the truss will approach a 2D anisotropic continuum. Simultaneously, the force polyhedron representing the structure's equilibrium converges to a continuous surface known as the Airy stress surface, portraying the stresses within the 2D body. In the following, we will delve into the equilibrium analysis of the 2D continuum, without explicitly considering compatibility conditions. The specific configuration of the limit truss and the stiffness of its rods will give rise to the local stiffness of the 2D continuum. It is noteworthy that the resulting equilibrium may not be achieved through elastic deformations of the limit truss. However, for quadrilateral trusses, as will be the case for principal symmetric structures, a unique equilibrium solution typically emerges when boundary loads are specified. Therefore, this solution can be attained through elastic deformations.

Let $D$ be a 2D continuum with loads and constraints applied on its boundary $\partial D$, and let it have a Cartesian reference system $xy$. At each point $p(x, y)$ within the continuum, the stress field can be described by the Cauchy stress tensor

$$S = \begin{pmatrix} \sigma_{xx} & \sigma_{xy} \\ \sigma_{xy} & \sigma_{yy} \end{pmatrix}.$$

Static equilibrium in the interior of the domain $D$ is expressed by $\operatorname{div} S = \mathbf{0}$, where the divergence is applied to both columns separately. In a simply connected domain, this implies existence of an Airy potential $\phi(x, y)$ such that

$$H_\phi = \begin{pmatrix} \phi_{,xx} & \phi_{,xy} \\ \phi_{,xy} & \phi_{,yy} \end{pmatrix} = \begin{pmatrix} \sigma_{yy} & -\sigma_{xy} \\ -\sigma_{xy} & \sigma_{xx} \end{pmatrix} = \tilde{S},$$

where $H_\phi$ is the Hessian of the function $\phi$ [16]. Here we indicate partial derivatives by a comma and subscripts, and with a tilde the adjoint matrix operation given by $\tilde{S} = R^T S R$.

The Airy stress potential can be seen as a surface $\Phi : z = \phi(x, y)$, often referred to as the *Airy stress surface*. Since stresses are determined by second derivatives of the Airy potential $\phi(x, y)$, potentials of the form $\phi'(x, y) = \phi(x, y) + c_1 x + c_2 y + c_3$ are associated with the same stress field, for all choices of $c_i$. Considering the transformation given by

$$z' = z + c_1 x + c_2 y + c_3, \tag{2}$$

it is important to note that this is not a Euclidean rigid body transformation. Consequently, Euclidean geometry should not be employed in the analysis of the Airy stress surface $\Phi$. Instead, one has to use a geometry in which the maps of Eq. (2) are rigid body transformations. This leads to *isotropic geometry*, which has been developed by K. Strubecker (see [17]). Strubecker has also been the first to realize the close connection between mechanical properties of a 2D stress field and geometric properties of the associated Airy surface $\Phi$ within isotropic geometry [6]. Isotropic geometry is based on the group of isotropic congruence transformations, which appear as Euclidean rigid body motions in the projection onto the $xy$-plane (top view). Hence, distances between points and angles between lines in isotropic space are just Euclidean distances and angles in the top view. Lines and planes parallel to the $z$-axis are called isotropic lines and planes, respectively.

In a 2D stress field, that lies in the plane $z = 0$, the stress tensor $S$ can be interpreted as follows: If we make an infinitesimal cut in the continuum at the point $p$ along a vector $\mathbf{a}$, the force acting across the cut is

$$\mathbf{f}(\mathbf{a}) = S R\, \mathbf{a}.$$

The corresponding stress vector (force per unit length) is given by

$$\boldsymbol{\sigma}(\mathbf{a}) = \frac{\mathbf{f}(\mathbf{a})}{\|\mathbf{a}\|}.$$

The normal stress across the cut $\mathbf{a}$, computed as

$$\sigma_n(\mathbf{a}) = \frac{\boldsymbol{\sigma}^T(\mathbf{a}) R\, \mathbf{a}}{\|\mathbf{a}\|} = \frac{\mathbf{a}^T H_\phi\, \mathbf{a}}{\mathbf{a}^T \mathbf{a}}, \tag{3}$$

corresponds to the isotropic normal curvature $\kappa_n^{is}$ of the Airy stress surface in direction $\mathbf{a}$. Principal stress directions $\mathbf{e}_1$, $\mathbf{e}_2$, given by the eigenvectors of $H_\phi$, correspond to isotropic principal curvature directions on the Airy surface $\Phi$. The associated principal stresses $\sigma_1$, $\sigma_2$ correspond to its isotropic principal curvatures.

In Euclidean geometry, the *osculating paraboloid* of a surface at a point $p$ is defined as the paraboloid that establishes second-order contact with the surface at $p$, its axis being normal to the surface at that specific point. This paraboloid reproduces the shape of the surface near this point up to variables of the second order. In the context of isotropic geometry, we can define the *isotropic osculating paraboloid* $\Pi$ of the Airy stress surface $\Phi$ as a paraboloid with a $z$-parallel axis making second-order contact with $\Phi$ at $p$. By intersecting the paraboloid $\Pi$ with a $xy$-parallel plane at a unit distance in $z$ direction from its vertex, we obtain a quadric curve called the *isotropic Dupin indicatrix*. If $\Pi$ is an elliptic paraboloid, the Dupin indicatrix is an ellipse where semi-axes $\mathbf{r}_1$, $\mathbf{r}_2$ point along the principal stress directions, with lengths $|\sigma_1|^{-\frac{1}{2}}$ and $|\sigma_2|^{-\frac{1}{2}}$ respectively (see Fig. 5). At a point $p$, an isotropic stress state is therefore characterized by a paraboloid of revolution, known in this context as *i-sphere*. This is represented by the equation

$$\Sigma : z = \frac{c_0}{2}(x^2 + y^2) + c_1 x + c_2 y + c_3,$$

where $c_0$ is its constant isotropic curvature. Any planar intersection of such an i-sphere is an *i-circle*: This is either a parabola with a $z$-parallel axis or an ellipse whose top view is a Euclidean circle.

### 2.3. Equilibrium of 2D quadrilateral networks

Let us now consider a 2D truss with a quadrilateral connectivity. At the limit of refinement, the edges of the truss will eventually converge to form a network of smooth curves on the domain $D$, as depicted in Fig. 3. The equilibrium of the network is now represented by its $z$-projection on the Airy stress surface $\Phi : z = \phi(x, y)$. To form a force polyhedron, this projected network should span infinitesimal planar faces on $\Phi$. Let $\mathbf{a}_1$, $\mathbf{a}_2$ be the tangent vectors of the two network curves passing through a point $p = (x, y) \in D$. Let us then consider the quadrilateral given by the points $\phi(p)$, $\phi(p+\mathbf{a}_1)$, $\phi(p+\mathbf{a}_2)$, and $\phi(p+\mathbf{a}_1+\mathbf{a}_2)$. Such a quadrilateral is planar if $\phi(p+\mathbf{a}_1+\mathbf{a}_2) = \phi(p+\mathbf{a}_1)+\phi(p+\mathbf{a}_2)$. A Taylor expansion tells us that

$$\phi(p + \mathbf{a}_1 + \mathbf{a}_2) - \phi(p + \mathbf{a}_1) - \phi(p + \mathbf{a}_2) = 2\, \mathbf{a}_1^T H_\phi\, \mathbf{a}_2 + o(\mathbf{a}_1 + \mathbf{a}_2)^2.$$

At a point $p$, two directions $\mathbf{a}_1$, $\mathbf{a}_2$ are then in equilibrium at the limit of refinement if

$$\mathbf{a}_1^T H_\phi\, \mathbf{a}_2 = 0. \tag{4}$$

Such directions are said to be *conjugate* to $H_\phi$. This result can also be interpreted informally as follows: Let us imagine to substitute the continuum at a point with two crossing rods $\mathbf{a}_1$ and $\mathbf{a}_2$. To insert the first rod, we have to make a cut $\mathbf{a}_1$ in the continuum. The resulting

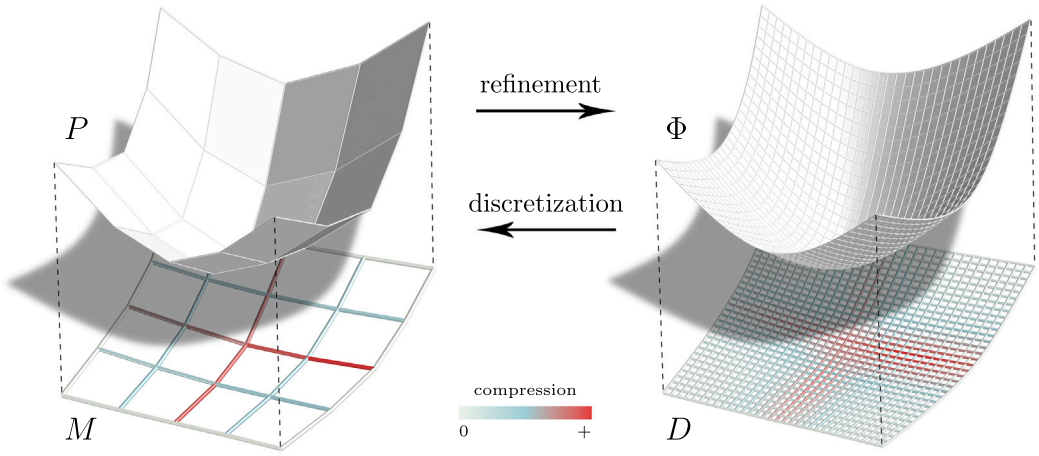


**Fig. 3.** On the *left*: A 2D quadrilateral truss $M$ and its Maxwell polyhedron $P$ representing the axial equilibrium. On the *right*: At the limit of refinement, the truss converges to a truss-like continuum D, and the corresponding Maxwell polyhedron converges to a network of curves which span planar faces on the Airy stress surface $\boldsymbol{\Phi}$.

force across it is $SR\,\mathbf{a}_1$. For axial force equilibrium, this force should point in the direction of the second rod $\mathbf{a}_2$, therefore $\mathbf{a}_1^T R^T S R\,\mathbf{a}_2 = \mathbf{a}_1^T H_\phi\,\mathbf{a}_2 = 0$. This condition is symmetric and entails equilibrium also for the insertion of the rod $\mathbf{a}_2$.

## 3. Principal symmetric trusses in 2D

In this section, we introduce the concept of principal symmetric structures in 2D and their characterization in isotropic geometry.

### 3.1. Stress symmetric networks in 2D

We look now for two directions $\mathbf{a}_1$, $\mathbf{a}_2$ such that the forces across these two cuts have the same magnitude, or rather $\|\boldsymbol{\sigma}(\mathbf{a}_1)\| = \|\boldsymbol{\sigma}(\mathbf{a}_2)\|$. To do this, let us first decompose the stress vector $\boldsymbol{\sigma}(\mathbf{a})$ into its normal component $\sigma_n$, given by Eq. (3), and its tangential component $\sigma_t$, given by

$$\sigma_t(\mathbf{a}) = \frac{\boldsymbol{\sigma}^T(\mathbf{a})\mathbf{a}}{\|\mathbf{a}\|}. \tag{5}$$

Let then $\mathbf{a}(\theta)$ be a direction that makes an angle $\theta$ with the principal stress direction $\mathbf{e}_1$, and define $\boldsymbol{\sigma}(\theta) = \boldsymbol{\sigma}(\mathbf{a}(\theta))$. Applying the tensor transformation law, the normal and tangential components of the stress vector can be now expressed as functions of the angle $\theta$ and of the principal stresses $\sigma_1$, $\sigma_2$ as follows:

$$\begin{aligned}\sigma_n(\theta) &= \sigma_1 \cos^2\theta + \sigma_2 \sin^2\theta,\\ \sigma_t(\theta) &= (\sigma_1 - \sigma_2)\sin\theta\cos\theta.\end{aligned} \tag{6}$$

These relations give rise to the well-known Mohr's circle, as depicted in Fig. 4. We can observe that the squared norm $\boldsymbol{\sigma}^2(\theta) = \sigma_n^2(\theta) + \sigma_t^2(\theta)$ is equal for couples of angles $\{\theta, -\theta\}$ – that is for directions that are symmetric to the principal stress directions $\mathbf{e}_1$, $\mathbf{e}_2$.

Two directions $\mathbf{a}_1$ and $\mathbf{a}_2$ that are symmetric to principal directions can be written as

$$\mathbf{a}_1 = a\mathbf{e}_1 + b\mathbf{e}_2 \quad \text{and} \quad \mathbf{a}_2 = a\mathbf{e}_1 - b\mathbf{e}_2, \tag{7}$$

where $a, b \in \mathbb{R}$. If we desire that $\mathbf{a}_1$ and $\mathbf{a}_2$ span a quad net in force equilibrium, they must fulfill the conjugacy Eq. (4). Therefore, substituting Eqs. (7), we get

$$\mathbf{a}_1^T H_\phi\,\mathbf{a}_2 = a^2\mathbf{e}_1^T H_\phi\,\mathbf{e}_1 - b^2\mathbf{e}_2^T H_\phi\,\mathbf{e}_2 = a^2\sigma_1 - b^2\sigma_2 = 0. \tag{8}$$

As first we note that the solution exists only if $\sigma_1$ and $\sigma_2$ have the same sign, i.e. for tension-only or compression-only stress states. Moreover,

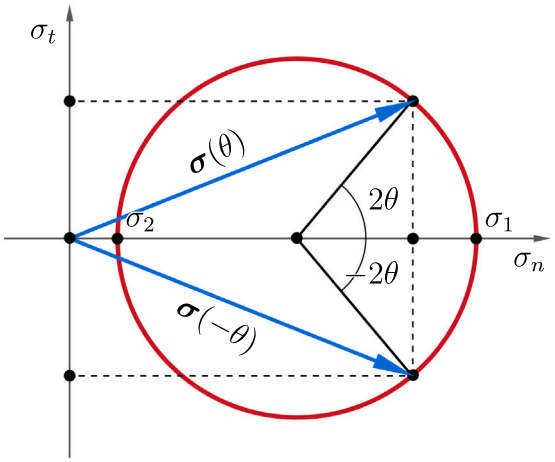


**Fig. 4.** Mohr's circle. In a $\sigma_n, \sigma_t$ plane, the components of the stress vector $\boldsymbol{\sigma}(\theta) = (\sigma_n(\theta), \sigma_t(\theta))^T$ form a circle with a diameter of $|\sigma_1 - \sigma_2|$, centered on the $\sigma_n$ axis. The stress vector $\boldsymbol{\sigma}(\theta)$ corresponds to a point that subtends an angle $2\theta$ with the principal stress direction associated with $\sigma_1$. It can be observed that stress vectors $\boldsymbol{\sigma}(\theta)$ and $\boldsymbol{\sigma}(-\theta)$ share the same magnitude.

we observe that the angle $\theta$ between the directions $\mathbf{a}_1$, $\mathbf{a}_2$ and the first principal direction $\mathbf{e}_1$ satisfies

$$\tan\theta = \pm\frac{b}{a} = \pm\sqrt{\frac{\sigma_1}{\sigma_2}}. \tag{9}$$

From Eq. (9), we observe that principal symmetric directions in equilibrium are aligned with the two diagonals of the axes rectangle of the Dupin indicatrix. We call these directions *characteristic stress directions*. By discretizing a characteristic stress network with a quadrilateral mesh, we obtain a principal symmetric gridshell in 2D. Some examples of principal symmetric gridshells for constant stress fields with different stress anisotropy are shown in Fig. 6.

Plugging Eq. (9) into Eqs. (6), we get

$$\boldsymbol{\sigma}^2 = \sigma_1\sigma_2. \tag{10}$$

We can see that, in a characteristic stress network, the norm of the stress vectors is everywhere constant for stress fields where $\sigma_1\sigma_2$ = constant, or equivalently, where $\det(H_\phi)$ = constant. We observe that such a stress state is characterized by an Airy stress surface of positive constant isotropic Gaussian curvature (see [17]).

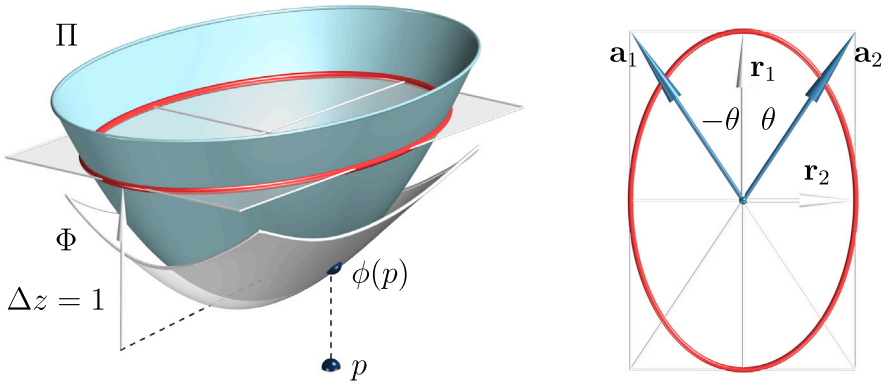


**Fig. 5.** Isotropic Dupin indicatrix. On the *left*: At a point $p$, the Dupin indicatrix is given by the intersection of the isotropic osculating paraboloid $\Pi$ of the Airy stress surface $\Phi$ with a plane at unit distance from its vertex. On the *right*: The characteristic stress directions $\mathbf{a}_1$, $\mathbf{a}_2$ point along the diagonals of the rectangle formed by the semi-axes $\mathbf{r}_1$, $\mathbf{r}_2$ of the Dupin indicatrix.

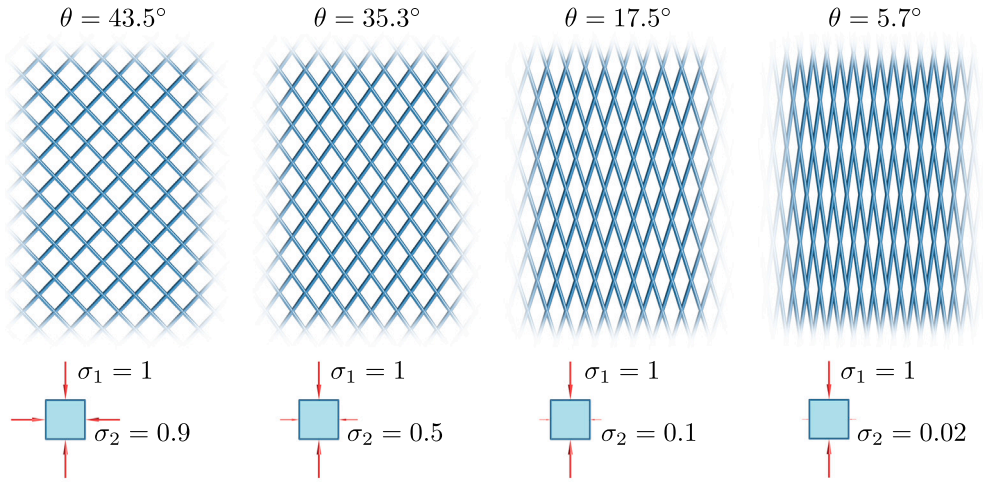


**Fig. 6.** Principal symmetric gridshells for constant 2D stress states. From *left* to *right*, the anisotropy of the principal stresses is increasing. Note that the rod layout is naturally disposed towards the major stress direction.

### 3.2. Stress symmetric networks in isotropic geometry

Let us now consider a curve on the Airy stress surface $\Phi$. At a point $p$, the *osculating i-circle* of the curve is defined as the ellipse with second order contact with the curve at $\phi(p)$ and whose top view is a Euclidean circle. Then, Meusnier's theorem in i-geometry, introduced in [17], says: All curves on a surface $\Phi$ which pass through a given point $p$ with the same tangent $\mathbf{a}$, possess osculating i-circles at $\phi(p)$ which lie on an i-sphere $\Sigma$ called the *Meusnier i-sphere*. The Meusnier i-sphere is tangent to $\Phi$ at $\phi(p)$ and its i-radius equals $1/\sigma_n$, where $\sigma_n$ is the normal curvature (that coincides here with the normal stress) across the direction determined by $\mathbf{a}$.

Hence, if two curves on a surface $\Phi$ are symmetric with respect to principal curvature directions at a point $p$, they possess the same Meusnier i-sphere $\Sigma$ at $\phi(p)$ (see Fig. 7). Viewing $\Phi$ as a stress surface, we obtain a geometric characterization of directions which are symmetric with respect to principal stress directions.

## 4. Principal symmetric gridshells

We now extend the previous results to surface-like gridshells in axial force equilibrium, loaded at joints with forces along a $z$-axis. With a refinement process similar to the one described in the 2D case, such a structure will converge to a "truss-like membrane", where the stress state is represented in its tangent plane by the membrane stress tensor. If the gridshell has a quadrilateral connectivity, the rods will then converge to a network of curves on the membrane surface. The geometric and mechanical properties of this limit network can be analyzed with differential geometry and continuum mechanics. For a formal description of gridshells approaching membranes, see [8].

### 4.1. Equilibrium at the limit of refinement

Let us consider a membrane surface $S \in \mathbb{R}^3$, given as the graph of a function $S : z = s(x, y)$. At a point $p \in S$, let $\mathbf{a}_1, \mathbf{a}_2 \in \mathbb{R}^3$ be two vectors tangent to the surface, and let $\bar{\mathbf{a}}_1, \bar{\mathbf{a}}_2 \in \mathbb{R}^2$ be their projections in the $xy$-plane. The first fundamental form I of the surface parametrization, given by

$$\mathrm{I} = \begin{pmatrix} 1 + s_{,x}^2 & s_{,x}s_{,y} \\ s_{,x}s_{,y} & 1 + s_{,y}^2 \end{pmatrix},$$

defines the inner product

$$\langle \mathbf{a}_1, \mathbf{a}_2 \rangle = \bar{\mathbf{a}}_1^T \mathrm{I}\, \bar{\mathbf{a}}_2. \tag{11}$$

Let the surface $S$ be subject to a distributed load in $z$ direction $p_z(x, y)$, expressed per unit $xy$-area, and let $S$ be the membrane stress tensor. The projection of the stress tensor in the $xy$-plane, denoted as $\bar{S}$, is then given by $\bar{S} = \Delta S$, where $\Delta = \det(\mathrm{I})$. Here, the determinant $\sqrt{\Delta}$ of the first fundamental form can be computed as $\sqrt{\Delta} = 1/\cos\beta$, where $\beta$ is the inclination angle of the design surface's tangent plane against the $xy$-plane. Since loads act only in $z$ direction, the $xy$-component of

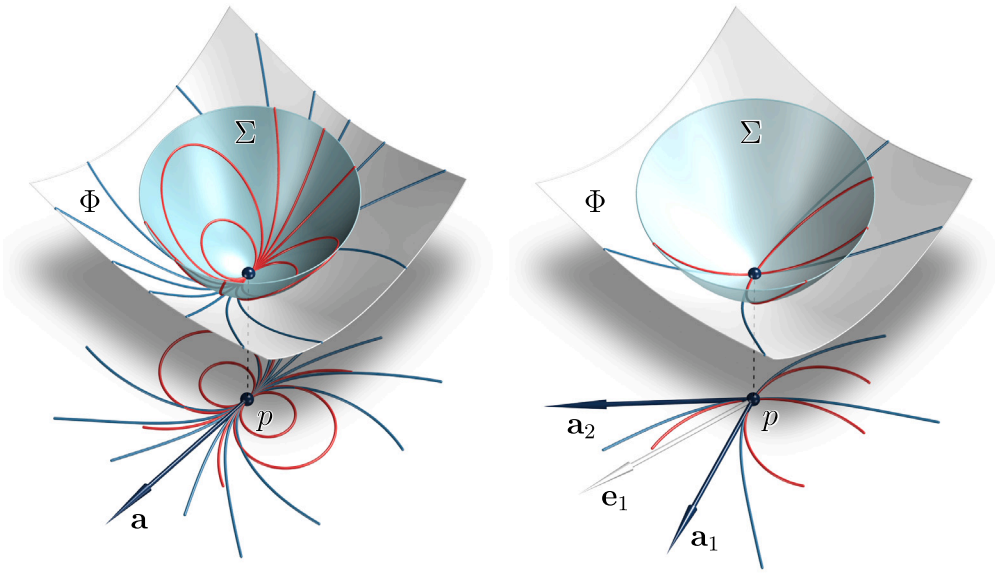


**Fig. 7.** Meusnier i-sphere $\Sigma$ of the Airy stress surface $\Phi$. On the *left*: At a point $p$, the osculating i-circles (*red*) of all surface curves that share the same tangent direction $\mathbf{a}$ lie on a i-sphere $\Sigma$. On the *right*: At a point $p$, the osculating i-circles (*red*) of two curves with tangents $\mathbf{a}_1$, $\mathbf{a}_2$ that are symmetric to the principal i-curvature direction $\mathbf{e}_1$ lie on the same i-sphere $\Sigma$. (For interpretation of the references to color in this figure legend, the reader is referred to the web version of this article.)

the equilibrium requires the projected stress tensor $\bar{S}$ to be divergence free. As in Section 2.2, this entails the existence of an Airy stress surface $\Phi : z = \phi(x, y)$, representing the $xy$-equilibrium, such that

$$\bar{S} = \tilde{H}_\phi = \begin{pmatrix} \phi_{,yy} & -\phi_{,xy} \\ -\phi_{,xy} & \phi_{,xx} \end{pmatrix}.$$

Being $H_s$ the Hessian of the surface $S$, given by

$$H_s = \begin{pmatrix} s_{,xx} & s_{,xy} \\ s_{,xy} & s_{,yy} \end{pmatrix},$$

the $z$-component of the equilibrium is described by the Pucher's equation

$$H_s : \tilde{H}_\phi + p_z = 0,$$

where $H_s : \tilde{H}_\phi = s_{,xx}\phi_{,yy} - 2s_{,xy}\phi_{,yy} + s_{,yy}\phi_{,xx}$ is a element-wise matrix multiplication.

The normal stress acting across a cut $\mathbf{a}$ in the surface is now computed as

$$\sigma_n(\mathbf{a}) = \frac{\bar{\mathbf{a}}^T \sqrt{\Delta} H_\phi \, \bar{\mathbf{a}}}{\bar{\mathbf{a}}^T \mathrm{I} \, \bar{\mathbf{a}}}. \tag{12}$$

Note that the principal stress directions and the corresponding principal stresses are now given by the eigenvectors and eigenvalues of $\sqrt{\Delta}\mathrm{I}^{-1} H_\phi$. We observe that the main difference between Eq. (12) and the 2D normal stress of Eq. (3) is that the inclination of the tangent plane of the design surface $S$ causes the appearance of the first fundamental form I. To adapt the isotropic geometry to the 3D membranes case, we need not use the canonical inner product in the $xy$-plane, but use the one induced by the first fundamental form of Eq. (11).

In this way, each point $p$ on the design surface $S$ determines via I a "locally adapted isotropic geometry". At each point $p$, such a geometry is related to the previously discussed one by applying an affine map in $xy$ and keeping $z$ unchanged. Hence all results are easily transferred. An i-sphere is now an elliptic paraboloid with equation of the form

$$\Sigma_p : z = \frac{c_0}{2}(\bar{\mathbf{x}}^T \mathrm{I} \, \bar{\mathbf{x}}) + c_1 x + c_2 y + c_3,$$

with $\bar{\mathbf{x}} = (x, y)^T$. Its intersections with non-isotropic planes are ellipses (i-circles) whose projections parallel to the $z$-axis into the tangent plane of the design surface $S$ at $p$ are Euclidean circles (see Fig. 8). Using the locally adapted isotropic geometry, the isotropic normal curvatures $\kappa_n$ on the stress surface $\Phi$ are related to the actual stresses on the design surface $S$ via

$$\sigma_n = \sqrt{\Delta}\kappa_n.$$

### 4.2. Quadrilateral gridshell networks

Let us consider now a quadrilateral gridshell that at the limit of refinement converges to a network of curves on $S$. Let $\mathbf{a}_1$ and $\mathbf{a}_2$ be the tangent vectors of the two network curves passing through a point $p$ of the surface, and let $\bar{\mathbf{a}}_1$ and $\bar{\mathbf{a}}_2$ be the projections of these vectors in the $xy$-plane. As in Eq. (4), horizontal equilibrium requires conjugacy of the projected directions to $H_\phi$.

We can also impose additional requirements on the network to facilitate the manufacturing process. For instance, we may seek a network with planar faces. As indicated in Eq. (4), this condition demands conjugacy with respect to the surface Hessian $H_s$. Including equilibrium, as shown in [7], this leads to conditions

$$\bar{\mathbf{a}}_1^T H_s \, \bar{\mathbf{a}}_2 = 0; \quad \bar{\mathbf{a}}_1^T H_\phi \, \bar{\mathbf{a}}_2 = 0, \tag{13}$$

which, together with a normalization constraint of vectors $\bar{\mathbf{a}}_1$ and $\bar{\mathbf{a}}_2$, give rise to four equations involving four variables. If at least one of the matrices $H_s$ or $H_\phi$ is invertible, both conditions are satisfied if $\bar{\mathbf{a}}_1$ and $\bar{\mathbf{a}}_2$ align with the eigenvectors of $H_s^{-1} H_\phi$ or $H_\phi^{-1} H_s$. If we additionally ask $\mathbf{a}_1$ and $\mathbf{a}_2$ to be orthogonal, and therefore $\bar{\mathbf{a}}_1^T \mathrm{I} \, \bar{\mathbf{a}}_2 = 0$, we have the condition that $\bar{\mathbf{a}}_1$ and $\bar{\mathbf{a}}_2$ must, at the same time, point along the eigenvectors of $\mathrm{I}^{-1} H_s$ and $\mathrm{I}^{-1} H_\phi$. This requires that the principal directions of stress and curvature coincide. Such a problem is over constrained and admits a solution only for a special class of membrane surfaces. A method for the design of such gridshells is described in [10].

### 4.3. Stress symmetric gridshell networks

Similarly to Section 3.1, we look now for two directions $\mathbf{a}_1$, $\mathbf{a}_2$ tangent to the surface $S$ at a point $p$ which are in equilibrium and along which the membrane stress vector has the same magnitude.

In this case, two tangent directions are symmetric with respect to the principal stress directions on $S$ if the corresponding directions on the Airy surface $\Phi$ have the same adapted Meusnier i-sphere. Note that angles in the adapted isotropic geometry agree with Euclidean angles

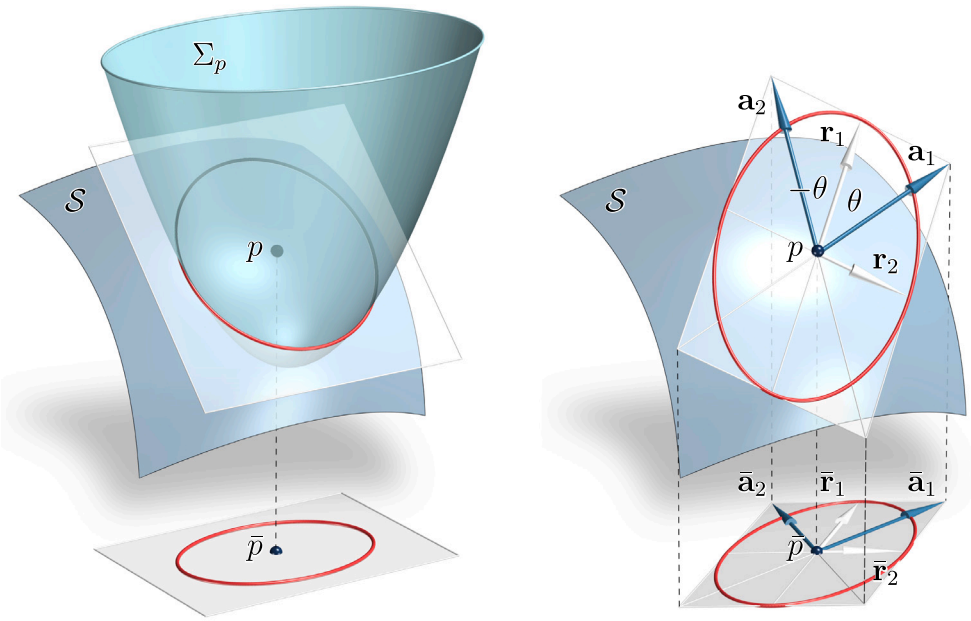


**Fig. 8.** On the *left*: The i-sphere $\Sigma_p$ in the adapted isotropic geometry. At a point $p$, an i-sphere intersects the tangent plane of the membrane surface $\mathcal{S}$ in a Euclidean circle, whose projection in the $xy$-plane is an ellipse. On the *right*: Principal symmetric directions at a point $p$ of a membrane $\mathcal{S}$. In *red*, the Dupin indicatrix of the adjoint stress tensor $\sqrt{\Delta \mathrm{I}^{-1}} H_\phi$ and its projection in the $xy$-plane are shown. (For interpretation of the references to color in this figure legend, the reader is referred to the web version of this article.)

in the corresponding tangent plane of the design surface. Therefore, Eqs. (6) and (9) are still valid, where the angles $\theta$ between the stress characteristic directions and the principal stress direction are Euclidean angles on the tangent plane of the design surface.

Let us now consider the Dupin indicatrix of the adjoint membrane stress on the tangent plane of $\mathcal{S}$. We have here the same conditions as described in Section 3.1, with stress characteristic directions being the diagonals of the principal axes rectangle, where now the principal stresses $\sigma_1, \sigma_2$ and the principal directions $\mathbf{e}_1, \mathbf{e}_2$ are the eigenvalues and eigenvectors of the adjoint stress tensor $\sqrt{\Delta \mathrm{I}^{-1}} H_\phi$. To compute the characteristic stress directions in our $xy$-parametrization, let us consider the eigenvectors of the adjoint stress tensor, denoted as $\bar{\mathbf{e}}_1$, $\bar{\mathbf{e}}_2$. The $xy$ projections of the semi-axes of the Dupin indicatrix are given by

$$\bar{\mathbf{r}}_1 = \frac{\bar{\mathbf{e}}_1}{\sqrt{|\bar{\mathbf{e}}_1^T H_\phi \bar{\mathbf{e}}_1|}}, \quad \bar{\mathbf{r}}_2 = \frac{\bar{\mathbf{e}}_2}{\sqrt{|\bar{\mathbf{e}}_2^T H_\phi \bar{\mathbf{e}}_2|}}.$$

As shown in Fig. 8, the $xy$ projection of the stress characteristic directions can be computed as $\bar{\mathbf{a}}_{1,2} = \bar{\mathbf{r}}_1 \pm \bar{\mathbf{r}}_2$. We observe that these directions are also conjugate to $H_\phi$: This can be seen considering that $(\bar{\mathbf{r}}_1 + \bar{\mathbf{r}}_2)^T H_\phi (\bar{\mathbf{r}}_1 - \bar{\mathbf{r}}_2) = \bar{\mathbf{r}}_1^T H_\phi \bar{\mathbf{r}}_1 - \bar{\mathbf{r}}_2^T H_\phi \bar{\mathbf{r}}_2$, and that $\bar{\mathbf{r}}_1^T H_\phi \bar{\mathbf{r}}_1 = \bar{\mathbf{r}}_2^T H_\phi \bar{\mathbf{r}}_2 = \pm 1$.

The stress conjugate gridshell network, as in the 2D case, is uniquely determined and exists solely for tension-only or compression-only membranes. A principal symmetric structure which additionally spans planar faces requires the conjugacy of the directions $\bar{\mathbf{a}}_1$, $\bar{\mathbf{a}}_2$ with respect to the surface Hessian $H_s$, as in Eq. (13). These networks exist only on a special class of membrane surfaces.

A particularly interesting structure would be one with constant forces in all the network. From Eq. (10), but considering the membrane principal stresses, we observe that this happens for networks where $\det(\sqrt{\Delta \mathrm{I}^{-1}} H_\phi) = \text{constant}$.

## 5. Design of principal symmetric structures

In this section, we outline a design workflow for the design of principal symmetric gridshells, summarized in Fig. 9.

### 5.1. Design of a compression-only (tension-only) membrane in equilibrium

As input, we need a compression-only or tension-only membrane in equilibrium. To compute it, we model the membrane $\mathcal{S}$ as a triangular gridshell truss, with loads applied on its vertices. The density of the triangular mesh should be chosen to match or be higher than the intended density of the final quadrilateral structure. We impose then the equilibrium at each unsupported vertex asking for compression-only or tension-only axial forces using the *force density method*: Being $w_{ij}$ the force density in the bar $\mathbf{v}_i - \mathbf{v}_j$, with positive values indicating compression, compressive (tensile) equilibrium at a vertex $\mathbf{v}_i$ is expressed as

$$\sum_{j \sim i} w_{ij}(\mathbf{v}_i - \mathbf{v}_j) + \mathbf{p}_i = 0, \quad \text{with} \quad w_{ij} > 0 \ (w_{ij} < 0), \tag{14}$$

where $\mathbf{p}_i$ is the load applied at the vertex $\mathbf{v}_i$. We address the form-finding task using the implementation proposed by Tang et al. [18], and compute the forces in the bars according to the resulting force densities. In this step, alternative form-finding methods which involve the computation of an Airy stress surface, based on NURBS surfaces [19] or radial basis functions [20], can be employed.

### 5.2. Computation of a principal symmetric network

Once we have a membrane in equilibrium, we estimate the stress tensor at vertices from the forces of incoming edges, using the normal cycle approach introduced by [21]. As shown in [10], one computes an extended stress tensor $S_e$ ($3 \times 3$ matrix with two eigenvectors in principal curvature direction and the third eigenvector, with eigenvalue close to zero, orthogonal to the surface) at a vertex $\mathbf{v}_i \in \mathbb{R}^3$ as follows:

$$S_e(\mathbf{v}_i) = \frac{1}{A_i} \sum_{j \sim i} w_{ij}(\mathbf{v}_i - \mathbf{v}_j)(\mathbf{v}_i - \mathbf{v}_j)^T,$$

where $A_i$ is the Voronoi area on the membrane mesh $\mathcal{S}$ associated with the vertex $\mathbf{v}_i$. The two swapped eigenvectors of $S_e(\mathbf{v}_i)$ lying in the tangent plane at $\mathbf{v}_i$, and the associated eigenvalues, are then used to compute the principal symmetric directions with Eq. (9).

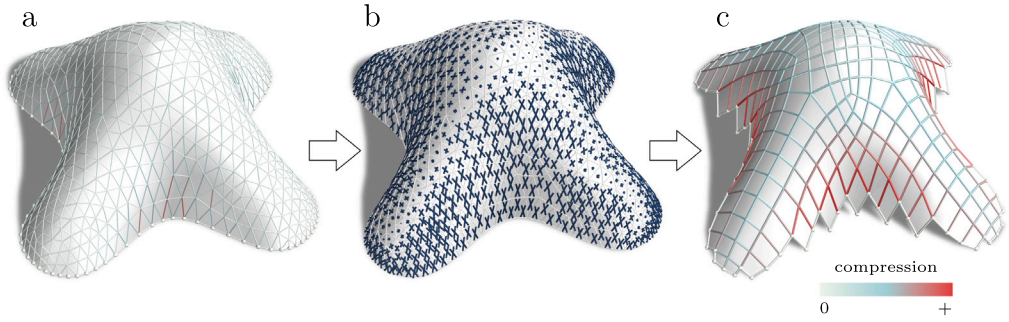


**Fig. 9.** Design pipeline. (a) A membrane shell in funicular equilibrium is given as input. To compute it, we use a triangular gridshell in compression-only or tension-only equilibrium. (b) We estimate the characteristic directions with Eq. (9). (c) We compute a quadrilateral mesh aligned with characteristic directions and we optimize the resulting gridshell for equal forces at nodes.

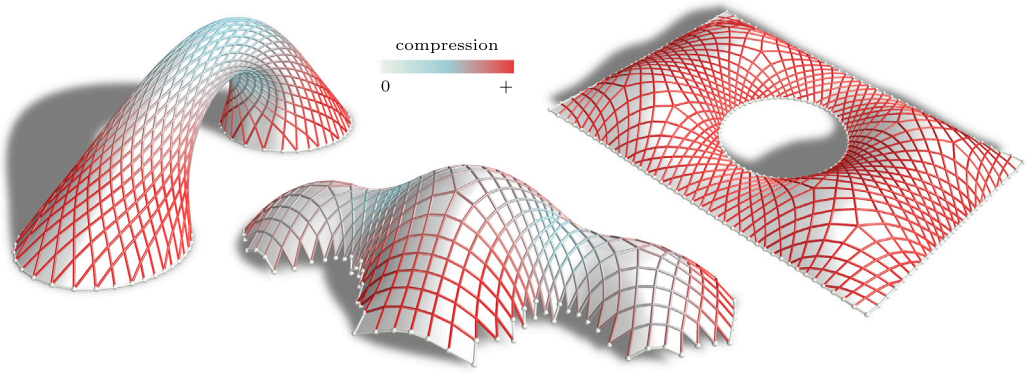


**Fig. 10.** Principal symmetric gridshells designed with our computational pipeline. Mesh singularities emerge at singular points of the principal stress lines of the limit membrane, coinciding with regions characterized by isotropic stress.

### 5.3. Quadrilateral remeshing

From the resulting directions, we extract then a quadrilateral mesh. Given that our hypotheses involve stresses, the achievement of accurate results hinges significantly on the condition that the edge lengths of this mesh are as uniformly distributed as possible. For this remeshing task, we use *mixed integer quadrangulation* [22]. This method requires as input an orthogonal cross field. Since principal symmetric directions are not orthogonal, we first transform the triangular mesh by moving its vertices such that the computed directions become orthogonal through optimization. An implementation of this transformation is described in [23]. We apply then mixed integer quadrangulation on the transformed mesh and map back the result on the original shape through barycentric coordinates.

### 5.4. Post-optimization

We finally optimize the quadrilateral mesh for equilibrium under vertical load with Eq. (14), additionally asking for equal forces at vertices. For that, at each unsupported vertex $i$ with connected vertices $j_1, j_2, j_3, j_4$, we define the force equalization energies

$$E_{\text{eq}} = \left( \|\mathbf{f}_{ij_k}\| - \|\mathbf{f}_{ij_l}\| \right)^2, \quad (k,l) \in \{(1,2),(2,3),(3,4),(4,1)\}.$$

We then minimize the sum of all energies $E_{\text{eq}}$ using a Levenberg–Marquardt algorithm, enabling the vertices of the mesh to move while maintaining proximity to the reference triangulated membrane. To ensure a uniform distribution of edge lengths, we can additionally minimize a fairness energy for each edge $i \sim j$, defined as $E_{\text{fair}} = \varepsilon \left( \|\mathbf{v}_i - \mathbf{v}_j\| - c \right)^2$, where $c$ is a coefficient subject to optimization and is equal for all edges. The parameter $\varepsilon$ denotes a small weight. During the optimization, we also minimize the graph Laplacian energy of the mesh, with a small weight, to ensure smoothness of mesh polylines (for details, see [18]).

Results are shown in Figs. 1, 2, 9, and 10. For all the presented examples, the structure is subjected to a constant area load along the vertical direction, and it is supported by pinned joints at the boundary vertices.

## 6. Conclusion and final remarks

In this study, we introduced principal symmetric gridshells, characterized by nearly equal axial forces at each joint. We demonstrated that these gridshells discretize a specific network of curves symmetrically aligned with the principal stress lines of either a tension-only or compression-only membrane. Additionally, we revealed insightful connections between this network and the isotropic geometry of the Airy stress surface. Finally, we outlined a method for computing a principal symmetric network on a membrane and extracting the corresponding principal symmetric gridshell.

Concerning manufacturing aspects, a potential extension of this work involves developing tools for designing principal symmetric structures with nearly constant forces in the rods, enabling the use of a single cross-section profile. As shown in Section 3, this can be achieved by designing membranes with a constant stress determinant.

A critical aspect to highlight is that principal symmetric gridshells generally do not span planar faces, presenting a challenge when covering them with panels made of rigid materials like glass. One plausible solution is to enable the design of membranes with stress characteristic directions that are conjugate to curvature. In this scenario, a remeshing along these directions would result in a principal symmetric gridshell with planar faces. The exploration of these extensions is deferred to future investigations.

## Declaration of competing interest

The authors declare that they have no known competing financial interests or personal relationships that could have appeared to influence the work reported in this paper.

## References


[1] Pottmann H, Liu Y, Wallner J, Bobenko A, Wang W. Geometry of multi-layer freeform structures for architecture. ACM Trans Graph 2007;26(3):65:1–65:11.

[2] Kilian M, Pellis D, Wallner J, Pottmann H. Material-minimizing forms and structures. ACM Trans Graph 2017;36(6):173:1–173:12.

[3] Adriaenssens S, Block P, Veenendaal D, Williams C, editors. Shell structures for architecture. Taylor & Francis; 2014.

[4] Fraternali F. A thrust network approach to the equilibrium problem of unreinforced masonry vaults via polyhedral stress functions. Mech Res Commun 2010;37(2):198–204.

[5] Block P, Ochsendorf J. Thrust network analysis: A new methodology for three-dimensional equilibrium. J Int Assoc Shell Spatial Struct 2007;48(3):167–73.

[6] Strubecker K. Airy'sche spannungsfunktion und isotrope differentialgeometrie. Math Z 1962;78:189–98.

[7] Vouga E, Höbinger M, Wallner J, Pottmann H. Design of self-supporting surfaces. ACM Trans Graph 2012;31(4):87:1–87:11.

[8] Mitchell T. A limit of economy of material in shell structures (Ph.D. thesis), University of California, Berkeley; 2013.

[9] Michell AGM. The limits of economy of material in frame-structures. Philos Mag Ser 6 1904;8(47):589–97.

[10] Pellis D, Pottmann H. Aligning principal stress and curvature directions. In: Hesselgren L, et al., editors. Advances in architectural geometry 2018. Klein Publishing; 2018.

[11] Schling E, Schikore J, Oberbichler T. D-nets on rotational surfaces: equilibrium gridshell layout, symmetric to the principal stress directions. In: Proceedings of IASS annual symposia. (22):International Association for Shell and Spatial Structures (IASS); 2020, p. 1–13.

[12] Pottmann H, Eigensatz M, Vaxman A, Wallner J. Architectural geometry. Comput Graph 2015;47:145–64.

[13] Pellis D, Wang H, Kilian M, Rist F, Pottmann H, Müller C. Principal symmetric meshes. ACM Trans Graph 2020;39(4):127:1–127:17.

[14] Pellis D, Pottmann H. Principal symmetric structures. In: Gabriele S, et al., editors. Shell and spatial structures. Lecture notes in civil engineering, vol. 437, Springer; 2023.

[15] Maxwell JC. On reciprocal figures, frames, and diagrams of forces. Trans R Soc Edinb 1872;26:1–40.

[16] Airy GB. On the strains in the interior of beams. Proc R Soc Lond 1862;12:304–6.

[17] Strubecker K. Differentialgeometrie des isotropen Raumes. III. Flächentheorie. Math Z 1942;48(1):369–427.

[18] Tang C, Sun X, Gomes A, Wallner J, Pottmann H. Form-finding with polyhedral meshes made simple. ACM Trans Graph 2014;33(4):70:1–9.

[19] Miki M, Igarashi T, Block P. Parametric self-supporting surfaces via direct computation of airy stress functions. ACM Trans Graph 2015;34(4):89:1–89:12.

[20] Chiang Y-C, Borgart A. A form-finding method for membrane shells with radial basis functions. Eng Struct 2022;251:113514.

[21] Cohen-Steiner D, Morvan JM. Restricted delaunay triangulations and normal cycle. In: Proceedings of the nineteenth annual symposium on computational geometry. New York: ACM; 2003, p. 312–21.

[22] Bommes D, Zimmer H, Kobbelt L. Mixed-integer quadrangulation. ACM Trans Graph 2009;28(3):77:1–77:10.

[23] Liu D, Pellis D, Chiang Y-C, Rist F, Wallner J, Pottmann H. Deployable strip structures. ACM Trans Graph 2023;42(4):103:1–103:16.